

Effect of alginate size, mannuronic/guluronic acid content and pH on particle size, thermodynamics and composition of complexes with β -lactoglobulin

Stender, Emil G. P.; Khan, Sanaullah; Ipsen, Richard; Madsen, Finn; Hägglund, Per; Abou Hachem, Maher; Almdal, Kristoffer; Westh, Peter; Svensson, Birte

Published in:
Food Hydrocolloids

DOI:
[10.1016/j.foodhyd.2017.09.001](https://doi.org/10.1016/j.foodhyd.2017.09.001)

Publication date:
2018

Document Version
Peer reviewed version

Citation for published version (APA):
Stender, E. G. P., Khan, S., Ipsen, R., Madsen, F., Hägglund, P., Abou Hachem, M., Almdal, K., Westh, P., & Svensson, B. (2018). Effect of alginate size, mannuronic/guluronic acid content and pH on particle size, thermodynamics and composition of complexes with β -lactoglobulin. *Food Hydrocolloids*, 75, 157-163.
<https://doi.org/10.1016/j.foodhyd.2017.09.001>

General rights

Copyright and moral rights for the publications made accessible in the public portal are retained by the authors and/or other copyright owners and it is a condition of accessing publications that users recognise and abide by the legal requirements associated with these rights.

- Users may download and print one copy of any publication from the public portal for the purpose of private study or research.
- You may not further distribute the material or use it for any profit-making activity or commercial gain.
- You may freely distribute the URL identifying the publication in the public portal.

Take down policy

If you believe that this document breaches copyright please contact rucforsk@kb.dk providing details, and we will remove access to the work immediately and investigate your claim.

Effect of alginate size, mannuronic/guluronic acid content and pH on particle size, thermodynamics and composition of complexes with β -lactoglobulin

Emil G. P. Stender^a, Sanaullah Khan^{a,b}, Richard Ipsen^c, Finn Madsen^d, Per Hägglund^a, Maher Abou Hachem^a, Kristoffer Almdal^b, Peter Westh^e, and Birte Svensson^{a,*}

a. Department of Biotechnology and Biomedicine, Technical University of Denmark, Kgs. Lyngby, Denmark

b. Department of Micro- and Nanotechnology, Technical University of Denmark, Kgs. Lyngby, Denmark.

c. Department of Food Science, University of Copenhagen, Frederiksberg, Denmark.

d. DuPont Nutrition Biosciences Aps, Brabrand, Denmark.

e. Roskilde University, Department of Science, Systems and Models, Roskilde, Denmark.

*Corresponding author: Department of Biotechnology and Biomedicine, Technical University of Denmark.

Elektrovej 375, DK-2800 Kgs. Lyngby. email: bis@bio.dtu.dk; phone: +4545252740

Abstract

Alginate is an anionic polysaccharide capable of forming insoluble particles with proteins. Hence, alginate has potential as a protein carrier. However, the role of physical properties of the polysaccharide, such as degree of polymerization (DP_n) and mannuronic/guluronic acid ratio, remains to be fully explored. Particle formation of a high and a low molar mass alginate (ALG) with β -lactoglobulin (BLG) at pH 2–8 depends on the average DP_n (HMW-ALG: $1.59 \cdot 10^3$; LMW-ALG: $0.23 \cdot 10^3$) and the mannuronic/guluronic acid ratio (1.0; 0.6) as supported by using ManA₆ and GulA₆ as models. Dynamic light scattering (DLS) showed that particles of BLG with either of the two ALGs have essentially the same hydrodynamic diameter (D_H) at pH 3 and 2, while at pH 4 particles of LMW-ALG/BLG have larger D_H than of HMW-ALG/BLG. At pH 5–8 no significant particle formation was observed. ManA₆ did not form insoluble particles at pH 2–8, while GulA₆ formed insoluble particles, albeit only at pH 4. K_d was approximately 10-fold higher for LMW-ALG/BLG than HMW-ALG/BLG and 3 orders of magnitude higher for an alginate trisaccharide/BLG complexation as determined by isothermal titration calorimetry (ITC). The alginate trisaccharide did not form insoluble particles with BLG at pH 3 and 4, though interaction still occurred. ΔH_{app} and molar stoichiometry of BLG in the complexes with the two ALGs differed by a factor of 7, as did their DP_n , which thus affected the interaction strength, but not the BLG content. At pH 4 the BLG content doubled in the particle due to BLG dimerization. The findings emphasize the importance of DP_n , mannuronic/guluronic acid ratio and pH in formulations containing alginate/whey protein particles.

Alginate (ALG), a linear anionic polysaccharide and major component of the cell walls of brown algae, consists of the 1,4-linked C5 epimers, β -D-mannuronic acid (M or ManA) and α -L-guluronic acid (G or GulA) found in homo- or mixed blocks (Fig. 1) (Ci et al., 1999; Johnson, Craig, Mercer, & Chauhan, 1997; Morris, Rees, & Thom, 1980). ALG is extensively used in the pharmaceutical and food industries as a gelling and stabilizing agent (Ci et al., 1999; Johnson et al., 1997). Growing interest in nano- and micro-particles of food ingredients motivated investigations on complex formation between negatively charged polysaccharides and positively charged proteins (Aberkane, Jasniewski, Gaiani, Scher, & Sanchez, 2010; Du, Dubin, Hoagland, & Sun, 2014; Fuenzalida et al., 2016; Girard, Turgeon, & Gauthier, 2003a; Jones, Adamcik, Handschin, Bolisetty, & Mezzenga, 2010). Two types of phase separation can occur when mixing such components; repulsive phase separation known as thermodynamic incompatibility; and attractive phase separation known as thermodynamic compatibility (Doublier, Garnier, Renard, & Sanchez, 2000). The former takes place at high concentrations of neutral or similarly charged protein and polysaccharide and results in separation into a protein-rich and a polysaccharide-rich phase. By contrast, thermodynamic compatibility occurs when polysaccharide and protein carry opposite charge, polarity or similar hydrophobicity and separate into a protein/polysaccharide rich and a protein/polysaccharide poor phase or exist as one homogeneous phase (Doublier et al., 2000). β -lactoglobulin (BLG) is the predominant protein in whey, the major by-product of cheese making. ALG/BLG complexes can act as carriers for nutrients and nutraceuticals, e.g. folic acid and curcumin and increase colloidal stability during storage in aqueous solution (Hosseini, Emam-Djomeh, Sabatino, & Van der Meeren, 2015). ALG previously received interest as a protein carrier due to its ability to form stable particles with bovine serum albumin that maintained its conformational integrity as assessed by circular dichroism analysis after pH-induced dissociation of the particles above the protein pI (Zhao, Li, Carvajal, & Harris, 2009). The pH range suitable for formation of particles from oppositely charged polymer and protein molecules depends on protein pI and ionic strength, but not on mixing ratio and molar mass of the polysaccharide (Girard, Turgeon, & Gauthier, 2002; Weinbreck, de Vries, Schrooyen, & de Kruif, 2003). However, properties of polysaccharides in interaction with proteins such as protein affinity, complex size and amount of bound protein may depend on the DP_n (Hosseini et al., 2013; Wang, Kimura, Dubin, & Jaeger, 2000). If the polysaccharide is too short attractive phase separation will not occur (Li, Xia, & Dubin, 1994). The charge density of the protein is important for complexation (Kayitmazer, Seyrek, Dubin, & Staggemeier, 2003), and the charge density of the protein polymer binding site plays a key role for the strength of interaction (Comert, Malanowski, Azarikia, & Dubin, 2016). The chain flexibility of polyelectrolytes and effective charge density may also influence particle formation (Du et al., 2014; Kayitmazer, Koksai, & Iyilik, 2015). The charge density on alginate M blocks has recently been hypothesized to be less than that of G blocks (Hecht & Srebnik, 2016) which could also have an effect on particle formation (Fuenzalida et al., 2016). Here it is hypothesized that the average chain length, as well as M/G ratio of ALG affect parameters governing particle formation with BLG, such as strength of interaction and molar stoichiometry of BLG and ALG and thereby the particle size. The effect of ALG DP_n and M/G-ratio on interaction with BLG was monitored by dynamic light scattering, turbidity and isothermal titration calorimetry at pH 2–9.

2. Materials and methods

2.1 Materials

BLG isoform A was purified in-house from raw milk (Kristiansen, Otte, Ipsen, & Qvist, 1998) and found to be > 95 % pure as assessed by SDS-PAGE. High (HMW) and low (LMW) molar mass sodium alginates (ALGs) were produced by DuPont Nutrition and Health. HMW-ALG has number weighted average molecular mass (\overline{M}_n) = 280 kDa, M/G ratio = 1.0 and polydispersity = 1.2. LMW-ALG has \overline{M}_n = 40 kDa, M/G ratio = 0.6 and polydispersity = 2.6 as analyzed (DuPont A/S) by SEC coupled to Multi Angle Light Scattering (\overline{M}_n and polydispersity) and FTIR spectroscopy (M/G ratio). Sodium salts of hexa-mannuronic acid (ManA₆) and hexa-guluronic acid (GulA₆) were purchased from Carbosynth (United Kingdom). All buffer components were of analytical grade.

2.2. Methods

2.2.1 Sample preparation

BLG in milliQ water (270 μM) was prepared by stirring (150 rpm, overnight, room temperature (RT)), centrifuged (12,000 g, 20 min, 20 °C) and filtrated (0.45 μm filter; Frisette ApS, Denmark); the concentration was determined spectrophotometrically at 280 nm using a molar extinction coefficient $\epsilon = 17,600 \text{ M}^{-1}\text{cm}^{-1}$ (Collini, D'Alfonso, & Baldini, 2000). HMW- and LMW-ALG (2 mg mL^{-1}) were prepared in milliQ water by stirring (150 rpm, overnight, RT) to ensure complete dispersion and filtrated (0.45 μm filter; Frisette ApS, Denmark). GuA₆ and ManA₆ (104 mM) were dissolved in milliQ water overnight and centrifuged (as above). BLG and ALG stocks were diluted with buffers (stock 100 mM, final 10 mM): glycine (pH 2), sodium citrate/citric acid (pH 3–6) and Tris-HCl (pH 7–9) and mixed to the desired ratios. For ITC BLG was dissolved in the respective buffers (200 μM), centrifuged (20,000 g, 20 min, 20 °C) and dialysed against 10 mM sodium citrate/citric acid (3 x 4 h, 4 °C, 6–8 kDa cutoff, SpectraPor membrane; Spectrum). ALGs (4 mg mL^{-1}) were dissolved in 10 mM sodium citrate/citric acid pH 3 or 4, centrifuged and dialysed (as above) to remove sodium ions added with the ALG. ALG tri-saccharide (ALGOS; see section 2.2.2) was dissolved in water (8.4 mM) and 100 mM sodium citrate/citric acid pH 3 or 4 was added to a final buffer concentration of 10 mM followed by centrifugation (as above).

2.2.2 Production, purification and characterization of ALGOS

LMW-ALG (10 mg mL^{-1}) in 50 mM Tris pH 7.2, 1 mg mL^{-1} BSA (100 mL) was added 10 U mL^{-1} of an endoacting alginate lyase from *Sphingomonas sp.* (Megazyme, United Kingdom) and incubated for 6.5 h at 40 °C under gentle mixing. The ALGOS obtained was desalted in milliQ water (HiPrep Desalt 26/10; GE Healthcare, Denmark) and purified by anion exchange chromatography (Mono Q 5/50 GL; GE Healthcare, Denmark) eluted by a 0–2 M NaCl linear gradient (2 h) in milliQ water at a flow rate of 1 mL min^{-1} . Eluted ALGOS was monitored by the absorbance at 235 nm (Park, Kam, Lee, & Kim, 2012). Fractions were pooled, added 0.5 M NaCl, filtered (3 kDa cut-off centrifugal filter; Amicon, Germany) to remove remaining protein, desalted as above and freeze dried (ScanVac FreezeSafe Freeze Dryer, Holm & Halby, Denmark). ALGOS samples were subjected to TLC (aluminium sheet Silica gel 60 WF254; Merck, Germany) developed twice in butanol:acetic acid:QH₂O (2:1:1) and stained by 10 % sulfuric acid, 80 % ethanol, 8 % H₂O and 2 % orcinol at 300 °C. MALDI-TOF MS was performed (Ultraflex II TOF/TOF; Bruker Daltonics) in positive ion linear mode using a polished steel TF MTP 384 target (Bruker Daltonics GmbH). Peak analysis of mass spectra was done using FlexAnalysis Version 3.3 (Bruker Daltonics GmbH).

2.2.3 Determination of alginate concentration and preparation of alginate standard

LMW-ALG (3 mg mL^{-1}) was dissolved in milliQ water, centrifuged and the supernatant dialyzed as above (3 x 4 h) against milliQ water. A 25 mL volumetric flask with glass stopper was cleaned with 96 % ethanol, heated (80 °C, 1 h), cooled to RT, weighed, filled with ALG solution, freeze-dried, desiccated (36 h, vacuum, RT; ME1 pump, Vacuubrand, United Kingdom), weighed, filled to the 25 mL mark with 10 mM sodium citrate/citric acid pH 4, and the LMW-ALG was dissolved under magnetic stirring (12 h) to give an ALG standard solution. The concentration of ALG used for ITC was determined by the phenol sulfuric acid method (Dubois, Gilles, Hamilton, Rebers, & Smith, 1956) with this ALG standard.

2.2.4 Turbidimetric and UV absorbance measurements

Turbidity of ALG/BLG mixtures (0.2 mg mL^{-1} /54 μM) was measured spectrophotometrically at 600 nm (Ultrospec pro 2100; Amersham Biosciences). Samples were centrifuged (20,000 g, 20 min, 20 °C; Eppendorf centrifuge 5417R, Denmark) and the absorbance of supernatants measured at 280 nm.

2.2.5 Dynamic light scattering

Particle size distribution of ALG (1 mg mL^{-1}), BLG (54 μM) and ALG/BLG (0.2 mg mL^{-1} /54 μM) mixtures was analysed by DLS (DLS instrument BI-200SM Brookhaven Instruments Corporation; USA) at a scattering angle of 90° at 23 °C. The distributions of mean apparent translational diffusion coefficients

(D_T) were determined by fitting DLS autocorrelation functions obtained with the instrument using non-negative constrained least-squares (NNLS). The distribution of mean apparent D_T was converted to the distribution of hydrodynamic diameter (D_H) using the Stokes-Einstein equation:

$$D_H = kT/3\pi\eta D_T$$

where k is the Boltzmann constant, T the absolute temperature, and η the solvent viscosity (0.93 mPa x s; assumed to be that of water at 296 K).

2.2.6 ζ -Potential of alginate and β -lactoglobulin

Electrophoretic mobility measurements were performed (Brookhaven 90Plus ZetaPALS Potential Analyzer; Brookhaven Instruments Corporation; USA) and the zeta potential (represented by ζ in millivolts) of BLG (1 mg·mL⁻¹) and LMW-ALG (1 mg·mL⁻¹), HMW-ALG (1 mg·mL⁻¹) was obtained from the electrophoretic mobility (μ_e) using Helmholtz-Smoluchowski equation:

$$\mu_e = \varepsilon\zeta/\eta$$

where ε is the dielectric constant (water) multiplied by the permittivity of vacuum, and η the solvent viscosity (0.93 mPa x s; assumed to be that of water at 296 K).

2.2.7 Isothermal titration calorimetry

ITC was used to determine the apparent dissociation constant (K_d) and the apparent change in enthalpy (ΔH_{app}) for complexation of ALGs and ALGOS with BLG at pH 3 and 4. Titrations were done with dialyzed ALG (1.5–3.5 mg mL⁻¹; 5–88 μ M, diluted in dialysis buffer) in the syringe and BLG (50–80 μ M, diluted in dialysis buffer) in the cell, by 26–40 injections each of 6 μ L (NanoITC2G; TA Instruments, USA) including an initial 3 μ L injection (deleted from the data set). A blank titration adding ALG into buffer was subtracted as heat of dilution. The conventional binding model for n identical sites was fitted to the resulting data (NanoAnalyze Data Analysis Version 3.4.0; TA instruments, USA). It is noted that this model relies on the mass action description of the binding process, which is only an approximation for the current system as the binding of BLG will modify the surface potential of ALG, hence resulting in continuous reduction of the affinity for BLG. K_d is thus not a true dissociation constant but an empirical measure of average affinity. K_d and ΔH_{app} were calculated by the program (NanoAnalyze software, TA). Errors are standard deviations for the regression analysis (NanoAnalyze software). This setup ensures similar ionic strength at all pH as opposed to particle formation by acidifying protein ALG mixtures. Purified ALGOS (in syringe: 4 mg mL⁻¹ = 7.6 mM) was added in 20 injections into BLG (in cell: 500 μ M), each of 2 μ L including an initial 0.4 μ L injection (excluded from the data set) (ITC200; Thermo Scientific, USA). Thermograms were corrected for heat of dilution, obtained from a blank titration, and a one-site binding model was fitted to integrated and normalized binding data.

3. RESULTS AND DISCUSSION

3.1 ζ -potential of ALG and BLG

The ζ -potential was measured in order to determine the surface charge under conditions where particles are formed. ζ -potential is a measure of the electrokinetic potential, *i.e.* the difference in electric potential between the solvent and the stationary layer of solvent molecules bound to dissolved particles. A ζ -potential is relative to the surface charge of molecules in solution (Makino & Ohshima, 2010). HMW- and LMW-ALGs have \overline{M}_n of 280 kDa and 40 kDa with calculated average maximum number of negative charges at high pH of 1591 and 227 as derived from M and G of 194 Da and pK_a 3.38 and 3.65, respectively (Draget, Braek, & Smidrod, 1994). At pH 2 HMW- and LMW-ALGs have a ζ -potential of -36 and -19 mV, respectively, indicating a negative surface charge even at this low pH (Fig. 2), perhaps due to polycarboxylic acid effects on pK_a and reflecting inter- and intra-molecular hydrogen bonding and

electrostatic forces (Castaneda et al., 2009). The ζ -potential did not change at pH 4. The different pH required to change the ζ -potential of HMW-ALG (pH 5) and LMW-ALG (pH 6) may be due to their different M/G ratio. BLG displayed positive ζ -potential of +24 mV at pH 2, which decreased linearly with increasing pH to -19 mV at pH 9 and a ζ -potential of 0 mV being reached just below pH 5 in accordance with experimental and calculated (ProtParam) BLG pI values of 4.7–5.2 (Bromley, Krebs, & Donald, 2005; Das & Kinsella, 1989; Sawyer & Kontopidis, 2000) and 4.83, respectively. The data agree with the ζ -potential value reported (Harnsilawat, Pongsawatmanit, & McClements, 2006) to be 0 mV for BLG at pH 5 and negative for ALG of similar mass to HMW (216 kDa), respectively, in the same pH range as studied here. Overall BLG and ALG carry opposite charge below pH 5. Notably, the ζ -potential of HMW- and LMW-ALGs differs by a factor of 3, which is less than expected from the DP_n of the ALGs varying 7 fold. An explanation for this may be the difference in viscosity.

3.2 Turbidity and absorbance of ALG/BLG mixtures

The solubility of ALG/BLG complexes was assessed by turbidity (at 600 nm) and absorbance (at 280 nm) measurements. The turbidity increased below pH 5 and did not change above pH 5, indicating attractive electrostatic interactions of ALG and BLG, which carry opposite charge at pH < 5 (Fig. 2 and 3A). No increase in turbidity or decrease in absorbance was observed for samples containing BLG and no ALG (data not shown). Decrease in turbidity was observed for all samples at pH 2 relative to pH 4, suggesting dissociation of particles as confirmed by an increased amount of protein in solution after centrifugation. At pH 4 and 3 a large decrease of protein in solution indicated formation of insoluble ALG/BLG particles. The reported optimum at pH 3.65–3.8 for formation of ALG/BLG particles with ALG of similar molar mass (200 kDa) (Hosseini et al., 2013) agrees with the present finding of highest turbidity of ALG/BLG at pH 4 (Fig. 3A).

Addition of ManA₆ or GulA₆ to BLG resulted in negligible turbidity at pH 2–9, except at pH 4, where GulA₆ elicited higher turbidity than ManA₆, accompanied by significant decrease in the amount of soluble protein measured at 280 nm after centrifugation (Fig. 3B). No drop in soluble protein was observed at pH 4 for ManA₆/BLG. This suggests that ALG/BLG particle formation is driven by G rather than M, possibly reminiscent of the greater ability of GulA₆ to form particles with BLG (Fig. 3C,D), although relatively higher GulA₆ concentration was required compared to LMW- and HMW-ALG (supplementary Fig. S2). The same concentration of ManA₆ marginally increased turbidity without significant loss of soluble protein. Noticeably, even the hexa-saccharide can participate in insoluble particle formation with BLG. The greater ability of GulA₆ to form insoluble complexes than ManA₆ was confined to a narrow pH range compared to the ability of HMW- and LMW-ALG (Fig. 3A,B). ALGOS/BLG mixtures did not display any turbidity at pH 3 and 4 and remained in solution after centrifugation (A_{280} of ALGOS/BLG was 0.941 before and 0.934 after centrifugation). Poly-G blocks are known to form a “buckled”-chain conformation with higher affinity for calcium than other metal cations, whereas M rich regions or mixed M/G blocks do not discriminate between different metal cations (Wong, Preston, & Schiller, 2000). The charge density simply may be higher on the more rigid GulA₆ (Hecht & Srebnik, 2016) than on ManA₆. GulA₆ therefore is superior in neutralizing local surface charge on BLG leading to aggregates as when the overall charge is 0 at the protein pI. This is in line with the observation that polyelectrolyte flexibility and local charge density is important for binding (Du et al., 2014). ALG of 7 kDa and M/G ratio 5 was recently reported to bind lysozyme more weakly than ALG of 4 kDa and M/G ratio 1.42 (Fuenzalida et al., 2016). A similar effect of G blocks as seen with calcium/ALG and lysozyme/ALG interactions possibly occurs for ALG binding BLG.

3.3 Size of HMW- and LMW-ALGs/BLG particles

The average particle size distribution of ALG, BLG and their mixtures at pH 2–8 showed a maximum at pH 4 for ALG/BLG, as given by the hydrodynamic diameter (D_H) (Fig. 4). Lower D_H values at pH 3 and 2 were similar for particles of HMW-ALG/BLG and LMW-ALG/BLG. The particle size at pH 3 (1482 ± 93 nm and 1652 ± 92 nm for LMW and HMW respectively) is slightly smaller than observed previously (Qomarudin et al., 2015), which may be due to differences in ionic strength of the buffer. The particle formation begins at pH 5, where D_H increases slightly compared to the BLG control. D_H of ALG/BLG particles were smaller at pH 3 and 2 than pH 4, suggesting partial dissociation of particles at low pH as reflected by higher K_d and lower stoichiometry of ALG/BLG at pH 3 (Table 1). D_H is highest for LMW-ALG compared to HMW-ALG at pH 4 and 5 which may be due to the higher G content of LMW-ALG in agreement with formation of more insoluble complexes with BLG by GulA₆ than by ManA₆ at pH 4 (Fig.

3B,C). D_H increased marginally at pH 6–8 compared to the BLG control (likely due to the D_H being calculated as a single species) indicating no interaction and supporting that the interaction is ionic, as BLG and ALG both carry a negative net charge at pH 6–8 (Fig. 2). The HMW- and LMW-ALG controls displayed almost the same D_H at pH 2–8 with a slight increase at pH 8 (Fig. 4, bottom). This may stem from greater charge at higher pH and hence stronger repulsion between individual saccharide units/regions.

3.5 Isothermal titration calorimetry

The large differences in particle size of ALG/BLG complexes between pH 4 and 3 may reflect variation in affinity and molecular stoichiometry. At pH 3 HMW-ALG/BLG complex formation has 11-fold lower K_d of 23 ± 3 nM than K_d of 266 ± 48 nM with LMW-ALG, different from what is expected from the avidity effect, possibly due to the difference in M/G ratio. HMW-ALG binds 7.6 times more BLG than LMW-ALG, corresponding to their 7-fold difference in \overline{M}_n (Table 1). At pH 4 both the strength of interaction and the stoichiometry increased two-fold in accordance with the larger D_H compared to at pH 3 (Fig. 4). HMW- and LMW-ALGs both displayed exothermic ΔH_{app} of complex formation with BLG at pH 3 and 4 (Fig. 5). The ratio of ΔH_{app} of particle formation at pH 3 between HMW- and LMW-ALGs was 6.7 (-6271.0 ± 96.6 kJ mol⁻¹, -939.5 ± 27.4 kJ mol⁻¹) and at pH 4 6.6 (-6666.0 ± 125.0 kJ mol⁻¹, -1013.0 ± 24.0 kJ mol⁻¹) (Table 1) but when compared in terms of J g⁻¹ none of the observed enthalpy's are significantly different.

ΔH_{app} of binding is similar to that of complex formation reported for BLG and other polysaccharides. Thus ΔH_{app} was -75.7 kJ (mol galacturonic acid)⁻¹ for pectin/BLG interaction (Girard, Turgeon, & Gauthier, 2003b) and very large ΔH_{app} was found in related systems undergoing attractive phase separation (Aberkane et al., 2010; de Souza, Bai, Goncalves, & Bastos, 2009). When soluble protein and anionic polysaccharides interact below pI of the protein, particle size increases significantly (Fig. 4). This is accompanied by reduction of the solvent accessible surface area and hence the number of hydrogen bonds with solvent, which would add an enthalpy effect. If this, however, was the sole explanation for ΔH_{app} , the reaction, due to loss of hydrogen bonds, would be endothermic which was not the case (Fig. 5). Another effect on ΔH_{app} apart from the change in enthalpy of interaction is the amount of bound protein that leaves solution per molecule of ALG, which at both pH 3 and 4 are similar when expressed in terms of J g⁻¹. The strong exothermic signal could be the result of bringing separated opposite charges together, which may also explain that ΔH_{app} does not differ much between pH 3 and 4 in accordance with the ζ -potential of the ALGs not changing significantly in that pH range (Fig. 2).

Since ALGOS did not display any turbidity at pH 3 and 4 the interaction with BLG was confirmed by using ITC. ALGOS and BLG interact at pH 4 with $K_d = 568 \pm 40$ μ M and $\Delta H_{app} = -3.4 \pm 0.5$ kJ mol⁻¹ (Table 1) and at pH 3 with $K_d = 1028 \pm 203$ μ M, possibly reflecting this is closer to the pK_a of ALGOS. The different n values of 1.71 and 1.28 bound ALGOS molecules per BLG monomer at pH 3 and 4, respectively (Table 1), probably reflect the higher positive charge of BLG (Fig. 2) as well as the larger available surface area at pH 3, where monomeric BLG prevails (Sakurai, Oobatake, & Goto, 2001). ΔH_{app} seems unaffected by the pH difference as observed also with the two ALGs, but is much smaller than ΔH_{app} for the polysaccharides (Table 1). This may be due to particle formation not occurring with ALGOS. The much higher affinity of ALG than ALGOS for BLG at pH 4 and 3 suggested massively enhanced interaction of BLG with the polysaccharide, likely as reflecting an avidity effect. This confirms previous findings for lysozyme that the larger the ALG DP_n the higher the affinity for this positively charged protein (Fuenzalida et al., 2016). Along the same line, ΔH_{app} is much smaller for ALGOS than for ALGs. The formed ALGOS/BLG complexes at completion of the titration are soluble as assessed by turbidity and A_{280} measurements. This supports the hypothesis of Li et al. that if DP_n of a polyelectrolyte is too low, large particles are not formed with oppositely charged molecules (Li et al., 1994) even though interaction still occurs (Fig. 5C). In the present case a too low DP_n is < 6 as judged from the ManA₆ and Gula₆ BLG interactions.

LMW-ALG binds 15.0 ± 0.3 and 30.5 ± 0.5 BLG monomers at pH 3 and 4, respectively, while HMW-ALG binds 113.8 ± 1.1 and 238.6 ± 3.3 BLG monomers (Table 1). This two-fold difference in stoichiometry between pH 3 and 4, may reflect ALG binding with monomeric and dimeric form of BLG (Sakurai et al., 2001; Taulier & Chalikian, 2001), and suggests that one or more ALG binding sites are situated close to the BLG dimerization interface. If a binding site on BLG was located far from the dimerization interface the amount bound per monomer should be similar at pH 3 and 4, but if the binding site is close to the dimerization interface a BLG dimer can bind only one ALG molecule. This is further supported by the K_d value being 50 % at pH 4 compared to pH 3, as expected from the avidity effect of dimerization. Girard et al. previously suggested BLG residues 132–148 contain a pectin binding site (Girard et al., 2003a). When viewed in the quaternary structure of the BLG dimer (Brownlow et al., 1997), this region forms a cleft possibly functioning as a binding site located in the dimerization interface. Altogether, the particle size of

ALG/BLG particles is greatly affected by pH but unaffected by DP_n in the range pH 2–3. At pH 4 G-blocks have a greater tendency to form insoluble particles than M-blocks, which may explain why LMW/BLG particles are larger than HMW/BLG particles at pH 4. The range in which insoluble particles are formed also depends on DP_n with hexasaccharides only forming insoluble particles at pH 4 and trisaccharides (ALGOS) never forming insoluble particles which may have something to do with the strength of interaction as seen from the ITC analysis. The present results indicate that the ALG/BLG particle formation varies importantly within the pH 2–4 range, probably due to BLG dimerization and to the local availability of charges on ALG as well as effects arising from the M/G ratio.

4. Conclusion

DP_n of ALG has a prominent effect on affinity and molar binding stoichiometry of BLG as determined by ITC, showing that the stoichiometry for the LMW- and HMW-ALGs increases by a factor corresponding to their difference in DP_n . Small oligosaccharides interact with mM-affinity and do not form insoluble particles, but when binding is accumulated in case of polysaccharides, the combined interaction is in the nM-range and insoluble particles are formed. While the D_H of complexes was unaffected by ALG DP at pH 3 and 2, it was greatly influenced in the pH 3–5 range and insoluble ALG/BLG complexes appeared at pH 3 and 4. This warrants further study using the model ALGOS and BLG to localize binding sites by identifying BLG residues engaged in complex formation. The results underline the importance of considering DP_n , M/G ratio and pH when preparing formulations for dairy food products from ALG and whey proteins.

Acknowledgements

This work is supported by the Danish Council for Strategic Research to the project StrucSat [Grant no. 1308-00011B] and a third PhD stipend (to EPGS) from the Technical University of Denmark. The NanoITC 2G was granted by the Danish Council for Strategic Research [Grant no. 11-116772 to PW]. The ITC 200 was granted by the Carlsberg Foundation [Grant no. 2011_01_0598 to MAH].

References

- Aberkane, L., Jasniewski, J., Gaiani, C., Scher, J., & Sanchez, C. (2010). Thermodynamic characterization of acacia gum-beta-lactoglobulin complex coacervation. *Langmuir*, 26(15), 12523–12533. <https://doi.org/10.1021/la100705d>
- Bromley, E. H. C., Krebs, M. R. H., & Donald, A. M. (2005). Aggregation across the length-scales in beta-lactoglobulin. *Faraday Discussions*, 128, 13–27. <https://doi.org/10.1039/b403014a>
- Brownlow, S., Cabral, J. H. M., Cooper, R., Flower, D. R., Yewdall, S. J., Polikarpov, I., ... Sawyer, L. (1997). Bovine beta-lactoglobulin at 1.8 angstrom resolution - Still an enigmatic lipocalin. *Structure*, 5(4), 481–495. [https://doi.org/10.1016/S0969-2126\(97\)00205-0](https://doi.org/10.1016/S0969-2126(97)00205-0)
- Castaneda, C. A., Fitch, C. A., Majumdar, A., Khangulov, V., Schlessman, J. L., & Garcia-Moreno, B. E. (2009). Molecular determinants of the pK(a) values of Asp and Glu residues in staphylococcal nuclease. *Proteins-Structure Function and Bioinformatics*, 77(3), 570–588. <https://doi.org/10.1002/prot.22470>
- Ci, S. X., Huynh, T. H., Louie, L. W., Yang, A., Beals, B. J., Ron, N., ... Desai, N. P. (1999). Molecular mass distribution of sodium alginate by high-performance size-exclusion chromatography. *Journal of Chromatography A*, 864(2), 199–210. [https://doi.org/10.1016/S0021-9673\(99\)01029-8](https://doi.org/10.1016/S0021-9673(99)01029-8)
- Collini, M., D'Alfonso, L., & Baldini, G. (2000). New insight on beta-lactoglobulin binding sites by 1-anilinonaphthalene-8-sulfonate fluorescence decay. *Protein Science*, 9(10), 1968–1974.
- Comert, F., Malanowski, A. J., Azarikia, F., & Dubin, P. L. (2016). Coacervation and precipitation in polysaccharide-protein systems. *Soft Matter*, 12(18), 4154–4161. <https://doi.org/10.1039/c6sm00044d>

361 Das, K. P., & Kinsella, J. E. (1989). pH dependent emulsifying properties of beta-Lactoglobulin. *Journal of*
362 *Dispersion Science and Technology*, 10(1), 77–102. <https://doi.org/10.1080/01932698908943160>

363 de Souza, H. K. S., Bai, G., Goncalves, M. do P., & Bastos, M. (2009). Whey protein isolate-chitosan interactions: a
364 calorimetric and spectroscopy study. *Thermochimica Acta*, 495(1–2), 108–114.
365 <https://doi.org/10.1016/j.tca.2009.06.008>

366 Doublier, J. L., Garnier, C., Renard, D., & Sanchez, C. (2000). Protein-polysaccharide interactions. *Current Opinion*
367 *in Colloid & Interface Science*, 5(3–4), 202–214. [https://doi.org/10.1016/S1359-0294\(00\)00054-6](https://doi.org/10.1016/S1359-0294(00)00054-6)

368 Draget, K. I., Braek, G. S., & Smidrod, O. (1994). Alginic acid gels - the effect of alginate chemical-composition and
369 molecular-weight. *Carbohydrate Polymers*, 25(1), 31–38. [https://doi.org/10.1016/0144-8617\(94\)90159-7](https://doi.org/10.1016/0144-8617(94)90159-7)

370 Du, X., Dubin, P. L., Hoagland, D. A., & Sun, L. (2014). Protein-selective coacervation with hyaluronic acid.
371 *Biomacromolecules*, 15(3), 726–734. <https://doi.org/10.1021/bm500041a>

372 Dubois, M., Gilles, K. A., Hamilton, J. K., Rebers, P. A., & Smith, F. (1956). Colorimetric method for determination
373 of sugars and related substances. *Analytical Chemistry*, 28(3), 350–356.
374 <https://doi.org/10.1021/ac60111a017>

375 Fuenzalida, J. P., Nareddy, P. K., Moreno-Villoslada, I., Moerschbacher, B. M., Swamy, M. J., Pan, S., ... Goycoolea,
376 F. M. (2016). On the role of alginate structure in complexing with lysozyme and application for enzyme
377 delivery. *Food Hydrocolloids*, 53, 239–248. <https://doi.org/10.1016/j.foodhyd.2015.04.017>

378 Girard, M., Turgeon, S. L., & Gauthier, S. F. (2002). Interbiopolymer complexing between beta-lactoglobulin and
379 low- and high-methylated pectin measured by potentiometric titration and ultrafiltration. *Food*
380 *Hydrocolloids*, 16(6), 585–591. [https://doi.org/10.1016/S0268-005X\(02\)00020-6](https://doi.org/10.1016/S0268-005X(02)00020-6)

381 Girard, M., Turgeon, S. L., & Gauthier, S. F. (2003a). Quantification of the interactions between beta-lactoglobulin
382 and pectin through capillary electrophoresis analysis. *Journal of Agricultural and Food Chemistry*, 51(20),
383 6043–6049. <https://doi.org/10.1021/jf034266b>

384 Girard, M., Turgeon, S. L., & Gauthier, S. F. (2003b). Thermodynamic parameters of beta-lactoglobulin-pectin
385 complexes assessed by isothermal titration calorimetry. *Journal of Agricultural and Food Chemistry*, 51(15),
386 4450–4455. <https://doi.org/10.1021/jf0259359>

387 Harnsilawat, T., Pongsawatmanit, R., & McClements, D. J. (2006). Characterization of beta-lactoglobulin-sodium
388 alginate interactions in aqueous solutions: A calorimetry, light scattering, electrophoretic mobility and
389 solubility study. *Food Hydrocolloids*, 20(5), 577–585. <https://doi.org/10.1016/j.foodhyd.2005.05.005>

390 Hecht, H., & Srebnik, S. (2016). Structural characterization of sodium alginate and calcium alginate.
391 *Biomacromolecules*, 17(6), 2160–2167. <https://doi.org/10.1021/acs.biomac.6b00378>

392 Hosseini, S. M. H., Emam-Djomeh, Z., Razavi, S. H., Moosavi-Movahedi, A. A., Saboury, A. A., Atri, M. S., & Van der
393 Meeren, P. (2013). Beta-lactoglobuline-sodium alginate interaction as affected by polysaccharide
394 depolymerization using high intensity ultrasound. *Food Hydrocolloids*, 32(2), 235–244.
395 <https://doi.org/10.1016/j.foodhyd.2013.01.002>

396 Hosseini, S. M. H., Emam-Djomeh, Z., Sabatino, P., & Van der Meeren, P. (2015). Nanocomplexes arising from
397 protein-polysaccharide electrostatic interaction as a promising carrier for nutraceutical compounds. *Food*
398 *Hydrocolloids*, 50, 16–26. <https://doi.org/10.1016/j.foodhyd.2015.04.006>

399 Johnson, F. A., Craig, D. Q. M., Mercer, A. D., & Chauhan, S. (1997). The effects of alginate molecular structure and
400 formulation variables on the physical characteristics of alginate raft systems. *International Journal of*
401 *Pharmaceutics*, 159(1), 35–42. [https://doi.org/10.1016/S0378-5173\(97\)00266-4](https://doi.org/10.1016/S0378-5173(97)00266-4)

- Jones, O. G., Adamcik, J., Handschin, S., Bolisetty, S., & Mezzenga, R. (2010). Fibrillation of beta-lactoglobulin at low pH in the presence of a complexing anionic polysaccharide. *Langmuir*, 26(22), 17449–17458. <https://doi.org/10.1021/la1026619>
- Kayitmazer, A. B., Koksai, A. F., & Iyilik, E. K. (2015). Complex coacervation of hyaluronic acid and chitosan: effects of pH, ionic strength, charge density, chain length and the charge ratio. *Soft Matter*, 11(44), 8605–8612. <https://doi.org/10.1039/c5sm01829c>
- Kayitmazer, A. B., Seyrek, E., Dubin, P. L., & Staggemeier, B. A. (2003). Influence of chain stiffness on the interaction of polyelectrolytes with oppositely charged micelles and proteins. *Journal of Physical Chemistry B*, 107(32), 8158–8165. <https://doi.org/10.1021/jp034065a>
- Kristiansen, K. R., Otte, J., Ipsen, R., & Qvist, K. B. (1998). Large-scale preparation of beta-lactoglobulin A and B by ultrafiltration and ion-exchange chromatography. *International Dairy Journal*, 8(2), 113–118. [https://doi.org/10.1016/S0958-6946\(98\)00028-4](https://doi.org/10.1016/S0958-6946(98)00028-4)
- Li, Y. J., Xia, J. L., & Dubin, P. L. (1994). Complex-formation between polyelectrolyte and oppositely charged mixed micelles - static and dynamic light-scattering study of the effect of polyelectrolyte molecular-weight and concentration. *Macromolecules*, 27(24), 7049–7055. <https://doi.org/10.1021/ma00102a007>
- Makino, K., & Ohshima, H. (2010). Electrophoretic mobility of a colloidal particle with constant surface charge density. *Langmuir*, 26(23), 18016–18019. <https://doi.org/10.1021/la1035745>
- Morris, E. R., Rees, D. A., & Thom, D. (1980). Characterization of alginic acid composition and block-structure by circular-dichroism. *Carbohydrate Research*, 81(2), 305–314. [https://doi.org/10.1016/S0008-6215\(00\)85661-X](https://doi.org/10.1016/S0008-6215(00)85661-X)
- Park, H. H., Kam, N., Lee, E. Y., & Kim, H. S. (2012). Cloning and characterization of a novel oligoalginate lyase from a newly isolated bacterium *Sphingomonas* sp MJ-3. *Marine Biotechnology*, 14(2), 189–202. <https://doi.org/10.1007/s10126-011-9402-7>
- Qomarudin, Q., Orbell, J. D., Ramchandran, L., Gray, S. R., Stewart, M. B., & Vasiljevic, T. (2015). Properties of beta-lactoglobulin/alginate mixtures as a function of component ratio, pH and applied shear. *Food Research International*, 71, 23–31. <https://doi.org/10.1016/j.foodres.2015.02.024>
- Sakurai, K., Oobatake, M., & Goto, Y. (2001). Salt-dependent monomer-dimer equilibrium of bovine beta-lactoglobulin at pH 3. *Protein Science*, 10(11), 2325–2335. <https://doi.org/10.1110/ps.17001>
- Sawyer, L., & Kontopidis, G. (2000). The core lipocalin, bovine beta-lactoglobulin. *Biochimica et Biophysica Acta-Protein Structure and Molecular Enzymology*, 1482(1–2), 136–148. [https://doi.org/10.1016/S0167-4838\(00\)00160-6](https://doi.org/10.1016/S0167-4838(00)00160-6)
- Taulier, N., & Chalikian, T. V. (2001). Characterization of pH-induced transitions of beta-lactoglobulin: Ultrasonic, densimetric, and spectroscopic studies. *Journal of Molecular Biology*, 314(4), 873–889. <https://doi.org/10.1006/jmbi.2001.5188>
- Wang, Y. L., Kimura, K., Dubin, P. L., & Jaeger, W. (2000). Polyelectrolyte-micelle coacervation: effects of micelle surface charge density, polymer molecular weight, and polymer/surfactant ratio. *Macromolecules*, 33(9), 3324–3331. <https://doi.org/10.1021/ma991886y>
- Weinbreck, F., de Vries, R., Schrooyen, P., & de Kruif, C. G. (2003). Complex coacervation of whey proteins and gum arabic. *Biomacromolecules*, 4(2), 293–303. <https://doi.org/10.1021/bm025667n>
- Wong, T. Y., Preston, L. A., & Schiller, N. L. (2000). Alginate lyase: review of major sources and enzyme characteristics, structure-function analysis, biological roles, and applications. *Annual Review of Microbiology*,

Zhao, Y., Li, F., Carvajal, M. T., & Harris, M. T. (2009). Interactions between bovine serum albumin and alginate: An evaluation of alginate as protein carrier. *Journal of Colloid and Interface Science*, 332(2), 345–353. <https://doi.org/10.1016/j.jcis.2008.12.048>

Figures:

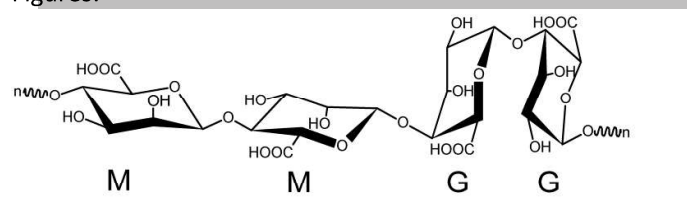


Fig 1. Chair conformation illustrating the structural motifs; 1,4-linked β -D-mannuronate block (left); α -L-guluronate block (right) and mixed M/G block (center) of ALG at low pH. n represents the continued polysaccharide.

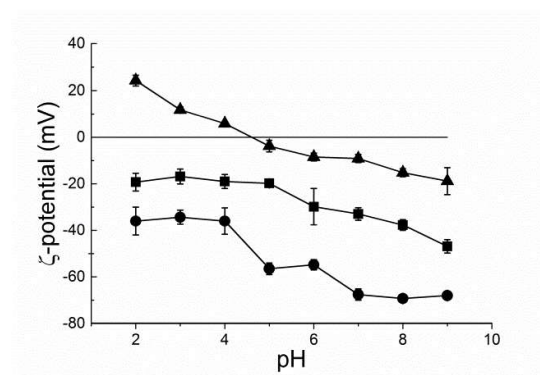


Fig 2. ζ -potential for LMW-ALG, HMW-ALG and BLG as a function of pH. HMW-ALG (circle), LMW-ALG (square), BLG (triangle).

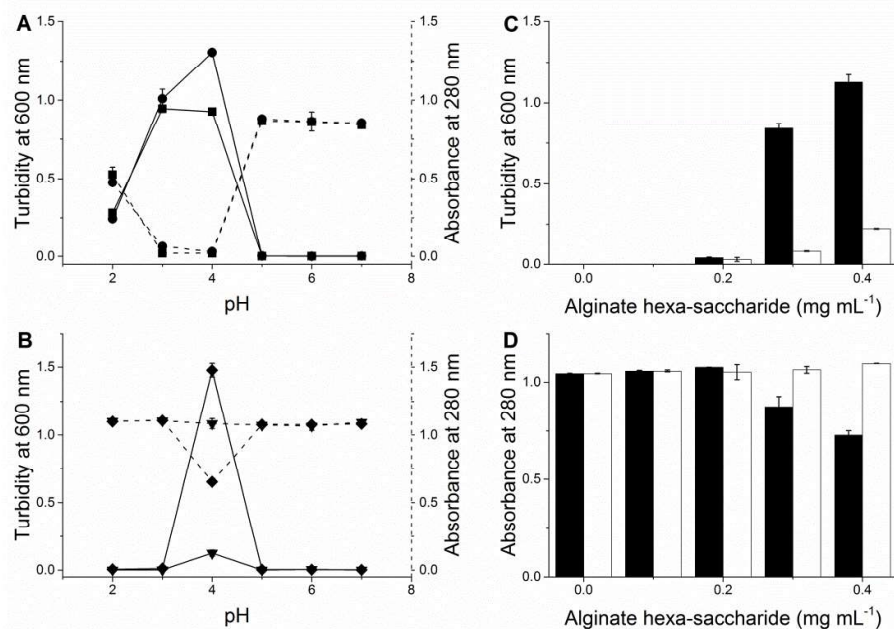
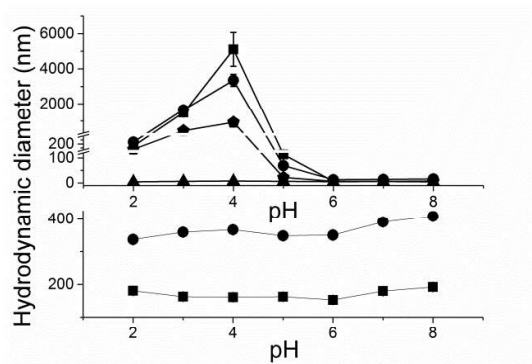


Fig 3. Turbidity and absorbance of ALG/BLG mixtures as a function of pH. Turbidity was measured at 600 nm after mixing (solid line). Absorbance of the supernatant was measured at 280 nm to determine the amount of protein remaining in solution (dashed line). A) 0.2 mg mL⁻¹ HMW- (circle) or LMW-ALG (square) mixed with 54 μ M BLG. B) 0.4 mg mL⁻¹ ManA₆ (diamond) or GulA₆ (upside down triangle) mixed with 1 mg mL⁻¹ BLG. C) Turbidity of 1 mg mL⁻¹ BLG mixed with varying concentration of GulA₆ (black) or ManA₆ (white) at pH 4. D) Absorbance after centrifugation of 1 mg mL⁻¹ BLG mixed with varying concentration of GulA₆ (black) or ManA₆ (white) at pH 4.



484 Fig 4. Hydrodynamic diameter (D_H) of ALGs, BLG and ALG/BLG mixtures. Top: Hydrodynamic diameter of
485 ALG/BLG as a function of pH. LMW-ALG (0.7 μM) and BLG (54 μM) (square), HMW-ALG (0.1 μM) and BLG
486 (54 μM) (circle), LMW-ALG (0.1 μM) and BLG (54 μM) (pentagon) and BLG (54 μM) (triangle). Bottom:
487 Hydrodynamic diameter of ALGs (1 mg mL^{-1}) as a function of pH. LMW-ALG (square), HMW-ALG (circle).
488

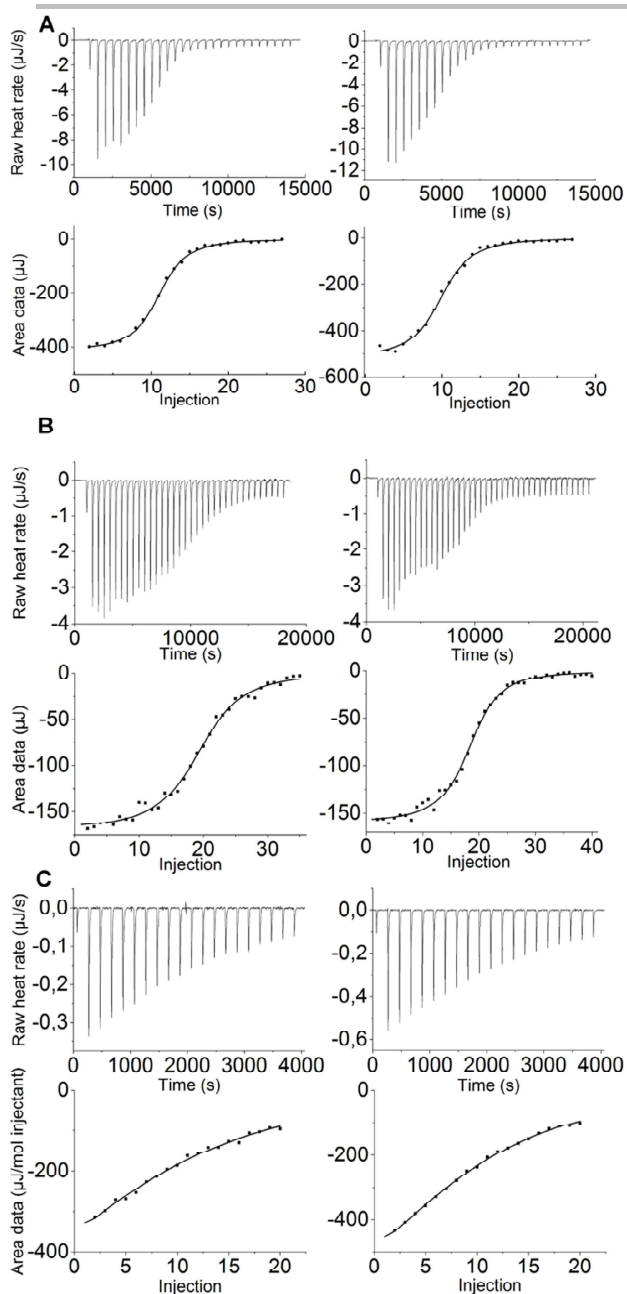
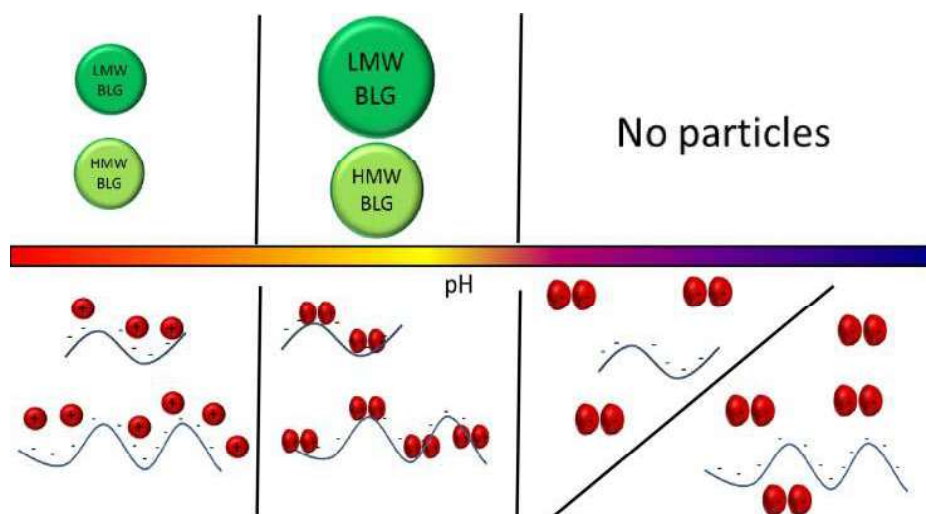


Fig 5. ITC of ALG/BLG complex formation at pH 3 and 4. For each experiment the upper portion shows the raw data with the baseline subtracted and the lower part shows the integrated peaks with the fitted one site binding model. A) HMW-ALG (left) LMW-ALG (right) titrated into BLG at pH 3. B) HMW-ALG (right) and LMW-ALG (left) titrated into BLG at pH 4. C) ALGOS titrated into BLG at pH 3 (left) and pH 4 (right).

500 Table 1. Thermodynamic parameters obtained for ALGs and BLG at pH 3 and 4 by using ITC (Fig. 5).
 501 *stoichiometry is reported as alginate oligomers bound per monomer of BLG. Numbers in brackets
 502 represent the data in terms of mass.

ALG	pH	K_d [nM] (g L ⁻¹)	n [BLG monomers/molecule ALG] (g BLG/g ALG)	ΔH_{app} [kJ mol ⁻¹] (J g ⁻¹)
HMW	3	23 ± 3 (6.44 · 10 ⁻³ ± 7.46 · 10 ⁻⁴)	113.8 ± 1.1 (7.44 ± 0.08)	-6271.0 ± 96.6 (-22.40 ± 0.35)
LMW	3	266 ± 48 (1.06 · 10 ⁻² ± 1.87 · 10 ⁻³)	15.0 ± 0.3 (6.88 ± 0.14)	-939.5 ± 27.4 (-23.41 ± 0.68)
ALGOS	3	1028 · 10 ³ ± 203 · 10 ³ (0.54 ± 0.11)	1.71 ± 0.2* (20.9 ± 0.06)	-3.1 ± 0.6 (-4.04 ± 0.40)
HMW	4	12 ± 2 (3.36 · 10 ⁻³ ± 5.14 · 10 ⁻⁴)	238.6 ± 3.3 (15.59 ± 0.21)	-6666.0 ± 125.0 (-23.81 ± 0.45)
LMW	4	119 ± 22 (4.76 · 10 ⁻³ ± 8.83 · 10 ⁻⁴)	30.5 ± 0.5 (13.94 ± 0.24)	-1013.0 ± 24.0 (-25.31 ± 0.62)
ALGOS	4	568 · 10 ³ ± 40 · 10 ³ (0.30 ± 0.02)	1.28 ± 0.0* (27.10 ± 0.00)	-3.4 ± 0.2 (-6.49 ± 0.33)

Graphical abstract



Highlights

- Particle size of alginate/ β -lactoglobulin complexes depends on pH
- Alginate/ β -lactoglobulin complex size depends on alginate M/G ratio and/or the molar mass
- Poly-guluronic acid has greater nanoparticle formation tendency than poly-mannuronic acid
- Formation of nanoparticles depends on alginate DP_n and pH
- With alginate oligosaccharide of DP_n = 3 no particles are formed but interaction occurs